

# Witnessing single-photon entanglement with local homodyne measurements

Olivier Morin\*,<sup>1</sup> Jean-Daniel Bancal\*,<sup>2</sup> Melvyn Ho,<sup>3</sup> Pavel Sekatski,<sup>2</sup> Virginia D'Auria,<sup>4</sup>  
Nicolas Gisin,<sup>2</sup> Julien Laurat,<sup>1</sup> and Nicolas Sangouard<sup>2</sup>

<sup>1</sup>Laboratoire Kastler Brossel, Université Pierre et Marie Curie,

Ecole Normale Supérieure, CNRS, 4 place Jussieu, 75252 Paris Cedex 05, France

<sup>2</sup>Group of Applied Physics, University of Geneva, CH-1211 Geneva 4, Switzerland

<sup>3</sup>Centre for Quantum Technologies, National University of Singapore, 3 Science Drive 2, Singapore 117543

<sup>4</sup>Laboratoire de Physique de la Matière Condensée, CNRS UMR 7336,

Université de Nice - Sophia Antipolis, Parc Valrose, 06108 Nice Cedex 2, France

(Dated: September 13, 2022)

Single-photon entangled states [1] constitute the simplest form of entanglement, yet they provide a valuable resource in quantum information sciences. Specifically, they lie at the heart of quantum networks, as they can be used for quantum teleportation [2, 3], swapped [4, 5] and purified [6, 7] with linear optics. The main drawback of such resource is the difficulty in measuring it. Here, we present and experimentally test the first operational witness suited for single-photon entanglement which relies only on local homodyning and does not require post-selection. Our results highlight the potential of hybrid methods, where discrete entanglement is characterized through continuous-variable measurements, in verifying the proper functioning of future quantum networks.

PACS numbers: 03.65.Ud

*Motivations* Quantum networks [8] provide broad capabilities, ranging from long distance quantum communication at large scales [4, 9], to the simulation of quantum many-body systems [10] in tabletop implementations. The envisioned networks are composed of nodes made with atoms where quantum information is generated and stored. Photons transport quantum states from site to site and the amazing properties of entanglement are used to efficiently connect the nodes. Remarkable progress has been made to store light efficiently [11, 12] for long times [13–16] and to generate entanglement between atomic ensembles [17–22]. Experimental capabilities are now advancing into a domain of rudimentary functionality for quantum nodes connected by quantum channels [25–28]. Surprisingly, the task of checking that a newly implemented quantum network performs well remains non-trivial.

In the past decade, a great number of architectures based on atomic ensembles and linear optics have been studied [29]. We now know that quantum networks based on single-photon entanglement, i.e. entangled states of the form

$$\frac{1}{\sqrt{2}} (|1\rangle_A |0\rangle_B + |0\rangle_A |1\rangle_B) \quad (1)$$

where  $A$  and  $B$  are two spatial modes sharing a delocalized photon, are very attractive: They require significantly fewer resources than the other architectures and are less sensitive to memory and photon detector inefficiencies [29]. Furthermore, they are efficient when combined with temporal multiplexing

[30]. However, such networks have a major drawback: The detection of single-photon entangled states is very challenging. One cannot resort, for example, to violating a Bell inequality given solely photon counting techniques.

Hitherto, there are two prescribed methods to detect single-photon entanglement. The first one converts two copies of a single-photon entangled state into one copy of two-particle entanglement. Starting from entanglement  $(|1\rangle_{A_1} |0\rangle_{B_1} + |0\rangle_{A_1} |1\rangle_{B_1}) \otimes (|1\rangle_{A_2} |0\rangle_{B_2} + |0\rangle_{A_2} |1\rangle_{B_2})$  between the modes  $A_1$  and  $B_1$  and between  $A_2$  and  $B_2$ , it basically consists of a post-selective projection onto the subspace with one excitation in each location, yielding  $|1\rangle_{A_1} |1\rangle_{B_2} + |1\rangle_{A_2} |1\rangle_{B_1}$  [4]. The latter is analogous to conventional polarization or time-bin entanglement. Since measurements in arbitrary bases are possible (by combining the modes  $A_1$ - $A_2$  on one side and  $B_1$ - $B_2$  on the other side, on beam-splitters with appropriate transmissions and phases), any witness suited for polarization or time-bin entanglement can be used to post-selectively detect the entanglement. Nevertheless, this approach is not fully satisfying conceptually because it relies on post-selection. Furthermore, for practical implementation, the need to create two copies requires twice the number of resources at each node.

The second method is based on quantum state tomography. For instance, one can reconstruct a reduced density matrix that corresponds to a projection of the full density matrix into a subspace with at most one photon locally. The presence of entanglement is then inferred from an entanglement measure computed from the reduced density matrix [18]. Specifically, this tomographic approach requires the knowledge of probabilities  $p_{mn}$  of having  $m$  photons in mode  $A$  and  $n$  in mode  $B$ , where  $m, n \in \{0, 1\}$ , and the visibility

---

\* These authors contributed equally to this work.

$V$  of the single-photon interference pattern obtained by combining the modes A & B into a beam-splitter. Although it has triggered highly successful experiments [18, 20–22], the approach presented in Ref. [18] cannot be directly used in large scale networks when one needs to check the entanglement between far away locations, since the knowledge of  $V$  relies on a joint measurement of A & B modes. Alternatively, one can use homodyne tomography to detect single-photon entanglement as reported in Ref. [23]. In this case, however, the corresponding state reconstruction relies on assumptions about the Hilbert space dimension [24].

*Principle* Here, we propose a witness uniquely suited for single-photon entanglement which does not need post-selection and relies on local measurements only. The basic principle is drawn in Fig. 1.

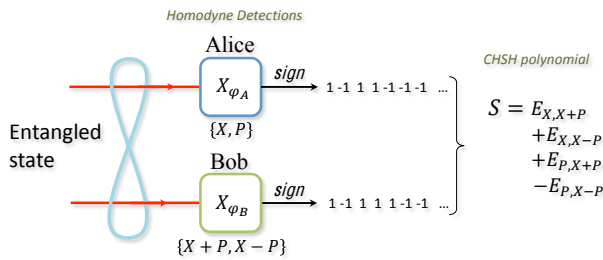


FIG. 1: Principle of the proposed entanglement witness for single-photon entanglement. Alice & Bob perform quadrature measurements on their respective quadrature basis, process the results using a sign binning and subsequently compute the CHSH value.

Two distant observers, Alice & Bob, share a quantum state. To check whether it is entangled, each of them randomly chooses a measurement among two quadratures,  $\{X, P\}$  for Alice and  $\{X + P, X - P\}$  for Bob. At each run, they obtain a real number. They then process the results to get binary outcomes using a sign binning, i.e. they attribute the result  $-1$  if the result is negative and  $+1$  otherwise. By repeating the experiment several times, Alice & Bob can compute the conditional probabilities  $p(a, b|x, y)$  where  $a, b \in \{-1, +1\}$ ,  $x \in \{X, P\}$  and  $y \in \{X + P, X - P\}$ . Substituting these probabilities by their values into the Clauser-Horne-Shimony-Holt (CHSH) [31] polynomial

$$S = E_{X, X+P} + E_{X, X-P} + E_{P, X+P} - E_{P, X-P}, \quad (2)$$

where  $E_{x,y} = \sum_{a,b \in \{-1, +1\}} p(a = b|x, y) - p(a \neq b|x, y)$ , they obtain a real number  $S$ .

The value of  $S$  can easily be obtained under the assumption that Alice & Bob have each a qubit. Indeed, in the Fock basis  $\{|0\rangle, |1\rangle\}$ , the measurement of the  $X$  quadrature with sign binning is equivalent to a noisy  $\sigma_x$

measurement [32, 33], i.e.

$$\int_{-\infty}^0 dx |x\rangle\langle x| - \int_0^{\infty} dx |x\rangle\langle x| = \sqrt{\frac{2}{\pi}} \sigma_x \quad (3)$$

and similarly, the  $P$  quadrature corresponds to  $\sigma_y$  with the same noise. For the setting choice  $\{X, P\}$  and  $\{X + P, X - P\}$ , the state (1) thus yields to  $S = 2\sqrt{2} \times \frac{2}{\pi} \approx 1.8$ . Furthermore, the maximum value that can be obtained with a separable state belonging to the subspace  $\{|0\rangle, |1\rangle\}^{\otimes 2}$  is  $S_{\text{sep}} = \sqrt{2} \times \frac{2}{\pi} \approx 0.9$  [34]. Since  $S$  is smaller than 2, the proposed CHSH-like test does not highlight the non-local characteristic of a single photon delocalized among two modes, but it does provide an attractive entanglement witness: If the measured CHSH value is larger than  $S_{\text{sep}}$ , Alice & Bob can conclude that they share an entangled state.

This holds for qubits only. In practice, however, the state describing the modes A & B includes multi-photon components, and does not reduce to a two-qubit state. We show below how the proposed entanglement witness can be extended to the general case where the shared bipartite state spans a Hilbert space of arbitrarily large dimension. First, we show how Alice & Bob can estimate the probability that their state lies out of a two-qubit space. We then demonstrate that this can be used to upper bound the maximal CHSH value that can be obtained with separable states. This leads to an entanglement witness uniquely suited for checking entanglement between two arbitrarily chosen nodes within a network.

*Bounding the Hilbert space dimension* Let us consider the case where Alice & Bob do not have qubits, but quantum states of arbitrary dimension. First, we ask them to bound the probability that at least one of their modes is populated with more than one photon ( $n_A \geq 2 \cup n_B \geq 2$ ) using local phase-averaged homodyne measurements. Specifically, the results of homodyning performed with phase averaged local oscillators uniquely determine the diagonal terms of each reduced density matrix, i.e. the probabilities  $p(n_A = j)$  ( $p(n_B = j)$ ) for having  $j$  photons in Alice's (Bob's) mode [35]. The joint probability  $p(n_A \geq 2 \cup n_B \geq 2) = p(n_A \geq 2) + p(n_B \geq 2) - p(n_A \geq 2 \cap n_B \geq 2)$  is then bounded by

$$p(n_A \geq 2 \cup n_B \geq 2) \leq 2 - \underbrace{\left( \sum_{j=0}^1 p(n_A = j) + p(n_B = j) \right)}_{=p^*}. \quad (4)$$

$p^*$  is usually non zero in practice, meaning that Alice & Bob's states do not reduce to qubits. We now show how the knowledge of  $p^*$  can be used to construct an operational witness for single-photon entanglement.

*Witnessing single-photon entanglement in a two-qudit space*

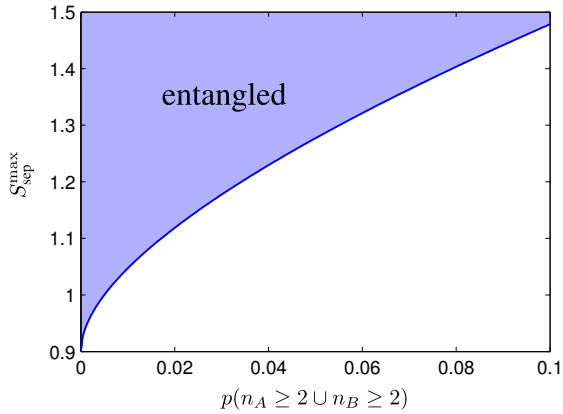


FIG. 2: Separable bound  $S_{\text{sep}}^{\text{max}}$  as a function of the probability that at least one of the two protagonists gets more than one photon  $p(n_A \geq 2 \cup n_B \geq 2)$ . From the measurement of an upper bound  $p^*$  on  $p(n_A \geq 2 \cup n_B \geq 2)$  obtained through local phase-averaged homodyne measurements, the blue curve allows one to know the maximum value of the CHSH polynomial  $S_{\text{sep}}^{\text{max}}$  that a separable state could reach. By performing a CHSH-like test based on homodyning, Alice & Bob get a CHSH value  $S_{\text{obs}}$ . If  $S_{\text{obs}} > S_{\text{sep}}^{\text{max}}$ , they can conclude that the state they share is entangled.

Consider the general case where  $p^* \neq 0$ , i.e.  $p(n_A \geq 2 \cup n_B \geq 2) \neq 0$  a priori. The state of Alice & Bob can be described by the density matrix

$$\rho = \begin{pmatrix} \rho_{n_A \leq 1 \cap n_B \leq 1} & \rho_{\text{coh}} \\ \rho_{\text{coh}}^\dagger & \rho_{n_A \geq 2 \cup n_B \geq 2} \end{pmatrix} \quad (5)$$

where  $\rho_{n_A \leq 1 \cap n_B \leq 1}$  denotes the  $4 \times 4$  block with at most one photon per mode,  $\rho_{n_A \geq 2 \cup n_B \geq 2}$  refers to the block where at least one of the two modes contains at least two photons and  $\rho_{\text{coh}}$  is associated to the coherence between these two blocks. Since  $\rho_{n_A \geq 2 \cup n_B \geq 2}$  possibly spans a Hilbert space of infinite dimension, there could be an infinite number of coherence terms. However, one can drastically reduce the number of these terms that give non-zero contribution to the CHSH polynomial by using a phase averaged homodyne detection at each location. Specifically, consider the case where Alice & Bob perform the measurements  $X_{\varphi_A} = \cos \varphi_A X + \sin \varphi_A P$  and  $X_{\varphi_B} = \cos \varphi_B X + \sin \varphi_B P$  respectively, where  $\varphi_A$  and  $\varphi_B$  are random variables such that  $\langle e^{ik\varphi_{A,B}} \rangle = 0$ ,  $k \in \mathbb{N}^*$  but where the phase difference  $\varphi_A - \varphi_B = \Delta\varphi$  is fixed. This only requires classical but not quantum communication, and hence can only decrease the entanglement that Alice & Bob potentially share. In particular, if Alice can choose a measurement among the two quadratures  $\{X_{\varphi_A^1}, X_{\varphi_A^2}\}$  and if Bob's choice reduces to one of the quadratures  $\{X_{\varphi_B^1}, X_{\varphi_B^2}\}$  such that  $\varphi_A^1 - \varphi_B^1 = -\frac{\pi}{4}$ ,  $\varphi_A^1 - \varphi_B^2 = \frac{\pi}{4}$ ,  $\varphi_A^2 - \varphi_B^1 = \frac{\pi}{4}$  and  $\varphi_A^2 - \varphi_B^2 = \frac{3\pi}{4}$ , we show in the Appendix A that the CHSH polynomial cor-

responding to the state (5) reduces to

$$S = \frac{16}{\sqrt{2}\pi} \Re \left[ \langle 01 | \rho_{n_A \leq 1 \cap n_B \leq 1} | 10 \rangle \right] \quad (6) \\ + \frac{8}{\pi} \left( \Re \left[ \langle 20 | \rho_{\text{coh}} | 11 \rangle \right] + \Re \left[ \langle 02 | \rho_{\text{coh}} | 11 \rangle \right] \right) \\ + S_{\rho_{n_A \geq 2 \cup n_B \geq 2}}$$

where  $\Re$  denotes the real part. The two following statements (i) the maximum value of  $S$  is  $2\sqrt{2}$  for any quantum state and (ii) the trace of  $\rho_{n_A \geq 2 \cup n_B \geq 2}$  is given by  $p(n_A \geq 2 \cup n_B \geq 2)$ , leave us with an upper bound on  $S$ , called  $S^{\text{max}}$  that is obtained by replacing the last term in Eq. (6) by  $2\sqrt{2} p(n_A \geq 2 \cup n_B \geq 2)$ .

For a given value of  $p(n_A \geq 2 \cup n_B \geq 2)$ ,  $S^{\text{max}}$  can be directly maximized over the set of states that remain positive under partial transposition (PPT) [1, 2] and satisfy the observed local photon number distributions, i.e.  $p_{00} + p_{10} + p_{01} + p_{11} = 1 - p(n_A \geq 2 \cup n_B \geq 2)$ . Since every separable state is PPT, this optimization provides a bound on the value of  $S^{\text{max}}$  achievable with separable states. Figure 2 shows the result of this optimization within the  $\{|0\rangle, |1\rangle, |2\rangle\}^{\otimes 2}$  subspace.

This provides a model independent witness [39] of entanglement: First, the protagonists determine the local photon-number distributions, from which they deduce an upper bound  $p^*$  on the joint probability to find more than one photon in at least one of the two modes  $p(n_A \geq 2 \cup n_B \geq 2)$ . Secondly, they use the results of these measurements to compute an upper bound on the maximum CHSH value  $S_{\text{sep}}^{\text{max}}(p^*)$  that can be reached with a separable state characterized by  $p(n_A \geq 2 \cup n_B \geq 2) \leq p^*$ . (See the Appendix A). Thirdly, they measure the CHSH value  $S_{\text{obs}}$  by randomly choosing measurements among  $\{X_{\varphi_A^1}, X_{\varphi_A^2}\}$  and  $\{X_{\varphi_B^1}, X_{\varphi_B^2}\}$  respectively and by subsequently computing the CHSH polynomial through Eq. (2). If  $S_{\text{obs}} > S_{\text{sep}}^{\text{max}}(p^*)$ , Alice & Bob can safely conclude that their state is entangled.

Note that a tighter bound can be obtained if  $S^{\text{max}}$  is maximized over the set of states with a positive partial transpose not only satisfying  $p_{00} + p_{10} + p_{01} + p_{11} = 1 - p(n_A \geq 2 \cup n_B \geq 2)$  but also that satisfy the locally measured probabilities  $p(n_A = j)$  ( $p(n_B = j)$ ) for having  $j = 0, 1$  photon in Alice's (Bob's) mode. These additional constraints have been taken into account for the computation of the separable bounds related to the experiment presented below (see Appendices).

*Proof-of-principle experiment* We now report on an experiment that uses the above mentioned approach to successfully witness single-photon entangled states. We start from a heralded single photon generated by a conditional preparation technique operated on a two-mode

squeezed vacuum emitted by a type-II optical parametric oscillator [5]. The entangled state shared by Alice & Bob is then obtained by sending the created photon into a beam-splitter. Specifically, by controlling the angle  $\theta$  of a half-wave plate relative to the axis of a polarizing beam-splitter (PBS), one creates a tunable single-photon entangled state  $\cos(2\theta)|0\rangle_A|1\rangle_B + \sin(2\theta)|1\rangle_A|0\rangle_B$  between the two output modes of the PBS, cf. Fig. 3.

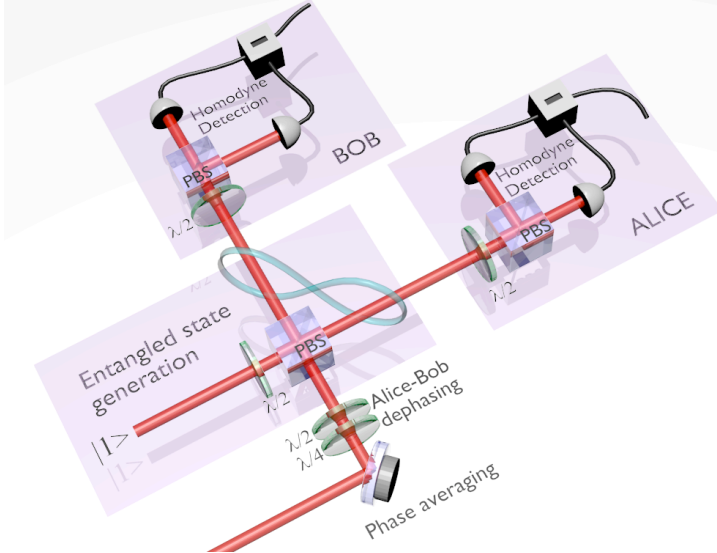


FIG. 3: Experimental setup. A tunable single-photon entangled state is created by sending a heralded single photon on a tunable beam-splitter based on a polarizing beam-splitter (PBS) and a half-wave plate ( $\lambda/2$ ). The proposed witness is then realized with two independent homodyne detections (Alice & Bob). The local oscillator is superposed to each modes via the first PBS. Its global phase is swept with a piezoelectric actuator in order to achieve the local phase averaging. The relative phase  $\Delta\varphi$  is set with a combination of a half-wave plate and a quarter-wave plate ( $\lambda/4$ ).

The local oscillators that Alice & Bob need to reveal entanglement, are obtained by impinging a bright beam on the second input of the PBS. The relative phase between Alice's and Bob's local oscillators  $\Delta\varphi$  is fixed by choosing an appropriate elliptical polarization of the bright beam just before the PBS [6]. In practice, the setting difference is calibrated by observing the dephasing of interference fringes (the quantum state is replaced here by a coherent state). A global phase averaging is obtained by sweeping a piezoelectric transducer located on the path of the bright beam before the PBS.

For each heralding event, Alice & Bob each obtain a real valued outcome which is extracted from homodyne photocurrents. Accumulating 200000 events for each quadrature relative measurements, they deduce the value of the CHSH polynomial  $S_{\text{obs}}$ . The same homodyne measurements also provide the local photon number distributions. The local probability distributions are

used to compute the separable bound  $S_{\text{sep}}^{\text{max}}$ . We emphasize that the separable bound is here obtained by maximizing the CHSH value over the set of separable states that fulfill the locally measured photon-number occupation probabilities  $p(n_A = j)$  and  $p(n_B = j)$  for having  $j = 0, 1$  photon in Alice & Bob's mode respectively. Furthermore, it takes several errors into account, for example, errors related to the quadrature measurement imperfections were considered (see Appendix B). The procedure is repeated for various angles  $\theta$  ranging from 0 to  $45^\circ$ . Fig. 4 shows the main result, i.e. the observed CHSH values and the separable bounds as a function of  $\theta$ . One sees that they both reach maximal values around  $\theta = 22.5^\circ$  where Alice & Bob ideally share a maximally entangled state. The small deviation between the observed value  $S_{\text{obs}}(\theta = 22.5^\circ) \approx 1.33$  and the CHSH value that would be obtained with a maximally entangled state (1.8) demonstrates that the overall source and detection efficiencies are very high ( $\approx 70\%$ ). Furthermore, the observed CHSH values are almost all larger than the separable bounds when dealing with entangled states ( $\theta \neq 0^\circ, 45^\circ$ ). This shows the great robustness of the proposed witness.

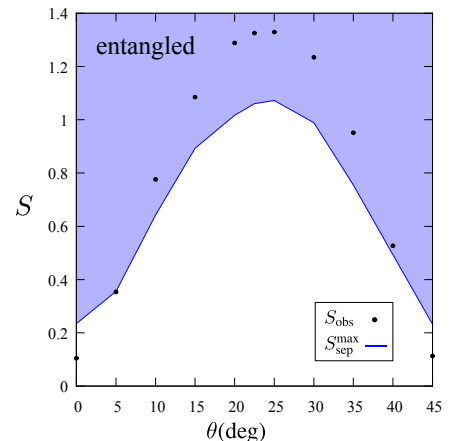


FIG. 4: Observed CHSH values  $S_{\text{obs}}$  (the size of points accounts for statistical errors) and separable bound  $S_{\text{sep}}^{\text{max}}$  as a function of beam-splitter angle  $\theta$ . If the observed CHSH value is higher than the separable bound, one can conclude the presence of entanglement with confidence. Note that the values of  $S_{\text{sep}}^{\text{max}}$  are lower than the ones presented in Fig. (2) because the optimization here presented, uses the knowledge of the locally measured probabilities  $p(n_A = j)$  ( $p(n_B = j)$ ) for having  $j = 0, 1$  photon in Alice's (Bob's) mode. This additional constraints leads to a tighter bound on  $S_{\text{sep}}^{\text{max}}$ .

*Conclusion* We have presented and experimentally tested a witness for single-photon entanglement. There are several reasons that make it attractive for practical implementation. First, it is not based on post-selection and hence, does not need extra copies of the state to be measured. Moreover, it involves a small number of measurements and could be used, without additional complications, to detect few-photon entanglement, obtained, for

example, by combining two single photons onto a beam-splitter. Although the relative phase of Alice's measurement device needs to be controlled with respect to Bob's one, the measurements are local. We thus believe that it will naturally find applications in long distance quantum communication, allowing users to check whether two remote nodes of a given quantum network are entangled. One important challenge in this context is to reveal the entanglement shared by a large number of parties. Finding Bell inequalities that could be used as witnesses for multi-partite single-photon entanglement is work for fu-

ture.

*Acknowledgments* We thank Mikael Afzelius, Cyril Branciard, Félix Bussi eres, Claude Fabre, Val erio Scarani, Rob Thew and Nuala Timoney for helpful discussions. We acknowledge support by the ERANET CHIST-ERA under the QScale project, by the EU project Qessence, from the Swiss NCCR-QSIT and from the National Research Fund and the Ministry of Education, Singapore. Julien Laurat is a member of the Institut Universitaire de France.

- 
- [1] S.J. van Enk, Phys. Rev. A **72**, 064306 (2005).  
[2] H.-W. Lee and J. Kim, Phys. Rev. A **63**, 012305 (2000).  
[3] E. Lombardi, F. Sciarrino, S. Popescu, F. De Martini, Phys. Rev. Lett. **88**, 070402 (2002).  
[4] L.-M. Duan *et al.*, Nature (London) **414**, 413 (2001).  
[5] F. Sciarrino, E. Lombardi, G. Milani, and F. De Martini, Phys. Rev. A **66**, 024309 (2002).  
[6] N. Sangouard *et al.*, Phys. Rev. A **78**, 050301(R) (2008).  
[7] D. Salart *et al.*, Phys. Rev. Lett. **104**, 180504 (2010).  
[8] H.J. Kimble, Nature **453**, 1023 (2008).  
[9] H.-J. Briegel, W. D ur, J.I. Cirac, and P. Zoller, Phys. Rev. Lett. **81**, 5932 (1998).  
[10] D. Illuminati, Nat. Phys. **2**, 803 (2006).  
[11] M.P. Hedges, J.J. Longdell, Y. Li and M.J. Sellars, Nature **456**, 1052 (2010).  
[12] M. Hosseini, B.M. Sparkes, G. Campbell, P.K. Lam and B.C. Buchler, Nat. Commun. **2**, 174 (2010).  
[13] J.J. Longdell, E. Fraval, M.J. Sellars, and N.B. Manson, Phys. Rev. Lett. **95**, 063601 (2005).  
[14] R. Zhang, S.R. Garner, and L. Vestergaard Hau, Phys. Rev. Lett. **102**, 033003 (2009).  
[15] F. Yuang, T. Mandel, C. Lutz, Z.-S. Yuan, and J.-W. Pan, Phys. Rev. A **83**, 063420 (2011).  
[16] A.G. Radnaev *et al.*, Nature Phys. **6**, 894 (2010).  
[17] B. Julsgaard, A. Kozhekin, and E.S. Polzik, Nature **413**, 400 (2001).  
[18] C.W. Chou *et al.*, Nature **438**, 828 (2005).  
[19] J. Simon, H. Tanji, S. Ghosh, and V. Vuleti c, Nature Phys. **3**, 765 (2007).  
[20] K.S. Choi, H. Deng, J. Laurat, and H.J. Kimble, Nature **452**, 67 (2008).  
[21] I. Usmani *et al.*, Nat. Photonics **6**, 234 (2012).  
[22] K.C. Lee *et al.*, Science **334**, 1253 (2011).  
[23] S.A. Babichev, J. Appel, and A.I. Lvovsky, Phys. Rev. Lett. **92**, 193601 (2004).  
[24] Note that it is possible to make homodyne tomography without assumptions on Hilbert space dimension provided that one assumes some regularity of the Wigner representation of the characterized state. These assumptions are often well justified but they are not necessary in the present proposal.  
[25] C.W. Chou *et al.*, Science **316**, 1316 (2007).  
[26] Z.-S. Yuan *et al.*, Nature **454**, 1098 (2008).  
[27] D.L. Moehring *et al.*, Nature **449**, 68 (2007).  
[28] S. Ritter *et al.*, Nature **484**, 195 (2012).  
[29] N. Sangouard, C. Simon, H. De Riedmatten and N. Gisin, Rev. Mod. Phys. **83**, 33 (2011).  
[30] C. Simon, H. De Riedmatten, M. Afzelius, N. Sangouard, H. Zbinden and N. Gisin, Phys. Rev. Lett. **98**, 190503 (2007).  
[31] J.F. Clauser, M. Horne, A. Shimony, R.A. Holt, Phys. Rev. Lett. **23**, 880 (1969).  
[32] M.T. Quintino *et al.*, J. Phys. A **45**, 215308 (2012).  
[33] N. Sangouard *et al.*, Phys. Rev. A **84**, 052122 (2011).  
[34] S.M. Roy, Phys. Rev. Lett. **94**, 010402 (2005).  
[35] M. Munroe *et al.*, Phys. Rev. A **52**, R924 (1995).  
[36] A. Peres, Phys. Rev. Lett. **77**, 1413 (1996).  
[37] M. Horodecki, P. Horodecki, and R. Horodecki, Phys. Lett. A **223**, 1 (1996).  
[38] J. Laurat, T. Coudreau, G. Keller, N. Treps, C. Fabre, Phys. Rev. A **71**, 022313 (2005).  
[39] The witness does not require that one knows the way the state has been created. However, it requires that Alice & Bob devices perform the desired measurements.  
[40] O. Morin, V. D'Auria, C.Fabre, J. Laurat, in preparation.

## Appendix A: Witnessing single-photon entanglement in qudit spaces: Theory

If Alice & Bob can guarantee that they perform measurements on qubits, they can witness entanglement by simply performing a Bell-like test by randomly choosing settings among two quadratures,  $\{X, P\}$  for Alice and  $\{X + P, X - P\}$  for Bob. If the resulting CHSH value is larger than  $\sim 0.9$ , they can safely conclude that their state is entangled. In practice, however, it is challenging to show that the systems one is measuring are well described by qubits. Below, we detail the procedure to follow in the general case where Alice & Bob systems are not restricted to qubits.

### 1. CHSH polynomial for phase averaged homodyning

Let

$$\rho = \sum_{ijkl} c_{ijkl} |ij\rangle\langle kl|$$

be the state that Alice & Bob share,  $|ij\rangle$  describing the state with  $i$  photons in Alice's mode and  $j$  photons in Bob's one. Consider that the phase of local oscillators that are required for homodyning is locally random, i.e. Alice & Bob perform the measurements

$$\begin{aligned} X_{\varphi_A^\ell} &= \cos \varphi_A^\ell X + \sin \varphi_A^\ell P, \\ X_{\varphi_B^{\bar{\ell}}} &= \cos \varphi_B^{\bar{\ell}} X + \sin \varphi_B^{\bar{\ell}} P \end{aligned}$$

respectively, with  $\varphi_A^\ell$  and  $\varphi_B^{\bar{\ell}}$  random variables satisfying  $\langle e^{in\varphi_A^\ell} \rangle = \langle e^{in\varphi_B^{\bar{\ell}}} \rangle = 0$ , for all  $n \in \mathbb{N}^*$ . Furthermore, consider the phase difference  $\Delta\varphi^{\ell\bar{\ell}} = \varphi_A^\ell - \varphi_B^{\bar{\ell}}$  to be tunable such that Alice's possible measurements  $\{X_{\varphi_A^1}, X_{\varphi_A^2}\}$  are fixed relative to Bob's ones  $\{X_{\varphi_B^1}, X_{\varphi_B^2}\}$ . (Note that this randomization of the local oscillators' phase can only lower the entanglement between Alice & Bob in average, because this can be realized by local operations and classical communication. Namely, Alice & Bob could use a shared randomized local oscillator and subsequently choose a quadrature measurement locally). At each run, Alice & Bob obtain each a real number. They then process the results to get binary outcomes using a sign binning, i.e. they assign the result  $-1$  if the real number is negative and  $+1$  otherwise. By repeating this procedure many times, they can access the probability that both get  $+1$  for instance, knowing that they chose measurements  $X_{\varphi_A^\ell}$  and  $X_{\varphi_B^{\bar{\ell}}}$

$$\begin{aligned} p(+1, +1 | X_{\varphi_A^\ell}, X_{\varphi_B^{\bar{\ell}}}) &= \sum_{ijkl} \langle e^{i\varphi_B^{\bar{\ell}}(i+j-(k+l))} \rangle c_{ijkl} \\ &\times e^{i\Delta\varphi^{\ell\bar{\ell}}(i-k)} \int_0^\infty dx \phi_i(x) \phi_k(x) \\ &\times \int_0^\infty dy \phi_j(y) \phi_l(y) \end{aligned}$$

where  $\phi_i(x) = \langle x|i\rangle$ . One sees that the off-diagonal elements  $|ij\rangle\langle kl|$  with different numbers of photons ( $i + j \neq k + l$ ) do not contribute to the probabilities  $p(a, b | X_{\varphi_A^\ell}, X_{\varphi_B^{\bar{\ell}}})$ , with  $a, b = \{-1, +1\}$ . Furthermore, since for all  $n$  and  $m$  having the same parity,

$$\int_0^\infty dy \phi_n(y) \phi_m(y) = \int_{-\infty}^0 dy \phi_n(y) \phi_m(y) = \frac{1}{2} \delta_{n,m},$$

the terms  $c_{ijkl}$  for which either  $i-k$  or  $j-l$  is an odd number, have a zero contribution to the correlator

$$\begin{aligned} E_{X_{\varphi_A^\ell}, X_{\varphi_B^{\bar{\ell}}}} &= \sum_{a,b=\{-1,+1\}} p(a = b | X_{\varphi_A^\ell}, X_{\varphi_B^{\bar{\ell}}}) \\ &\quad - p(a \neq b | X_{\varphi_A^\ell}, X_{\varphi_B^{\bar{\ell}}}). \end{aligned}$$

Finally, one easily checks that the remaining  $c_{ijkl}$  terms satisfying

$$i + j = k + l, \quad (\text{A1})$$

$$|i - k| = 1 \pmod{2}, \quad (\text{A2})$$

$$|j - l| = 1 \pmod{2}, \quad (\text{A3})$$

yield

$$\begin{aligned} E_{X_{\varphi_A^\ell}, X_{\varphi_B^{\bar{\ell}}}} &= 4 \sum_{ijkl} c_{ijkl} \\ &\times \int_0^\infty dx \phi_i(x) \phi_k(x) e^{i\Delta\varphi^{\ell\bar{\ell}}(i-k)} \\ &\times \int_0^\infty dy \phi_j(y) \phi_l(y). \end{aligned}$$

Specifically, if  $\Delta\varphi^{11} = -\frac{\pi}{4}$ ,  $\Delta\varphi^{12} = \frac{\pi}{4}$ ,  $\Delta\varphi^{21} = \frac{\pi}{4}$  and  $\Delta\varphi^{22} = \frac{3\pi}{4}$ , the value of the CHSH polynomial

$$S = E_{X_{\varphi_A^1}, X_{\varphi_B^1}} + E_{X_{\varphi_A^1}, X_{\varphi_B^2}} + E_{X_{\varphi_A^2}, X_{\varphi_B^1}} - E_{X_{\varphi_A^2}, X_{\varphi_B^2}}$$

is given by

$$\begin{aligned} S &= 16 \sum_{ijkl} c_{ijkl} \cos\left((i-k)\frac{\pi}{4}\right) \\ &\times \int_0^\infty dx \phi_i(x) \phi_k(x) \cdot \int_0^\infty dy \phi_j(y) \phi_l(y). \end{aligned} \quad (\text{A4})$$

### 2. Optimizing the CHSH value over the set of separable states

Without loss of generality, Alice & Bob's state can be written as

$$\rho = \begin{pmatrix} \rho_{n_A \leq 1 \cap n_B \leq 1} & \rho_{\text{coh}} \\ \rho_{\text{coh}}^\dagger & \rho_{n_A \geq 2 \cup n_B \geq 2} \end{pmatrix} \quad (\text{A5})$$

where  $\rho_{n_A \leq 1 \cap n_B \leq 1}$  denotes the block with at most one photon per mode,  $\rho_{n_A \geq 2 \cup n_B \geq 2}$  refers to the block where at least one of the two modes is populated with more than one photon and  $\rho_{\text{coh}}$  is associated to the coherence between these two blocks. Taking the constraints (A1),(A2)

and (A3) into account and using the formula (A4), the corresponding CHSH polynomial reduces to

$$S = \frac{16}{\sqrt{2\pi}} \Re \left[ \langle 01 | \rho_{n_A \leq 1 \cap n_B \leq 1} | 10 \rangle \right] \quad (\text{A6})$$

$$+ \frac{8}{\pi} \left( \Re \left[ \langle 20 | \rho_{\text{coh}} | 11 \rangle \right] + \Re \left[ \langle 02 | \rho_{\text{coh}} | 11 \rangle \right] \right)$$

$$+ S_{\rho_{n_A \geq 2 \cup n_B \geq 2}}$$

where  $\Re$  denotes the real part and  $S_{\rho_{n_A \geq 2 \cup n_B \geq 2}}$  is associated to the CHSH value obtained from  $\rho_{n_A \geq 2 \cup n_B \geq 2}$ . The goal is now to optimize  $S$  over the set of separable states.

Since the maximum quantum value of  $S$  is  $2\sqrt{2}$ , the last term of (A6) is upper bounded by  $2\sqrt{2} \times p(n_A \geq 2 \cup n_B \geq 2)$ , where  $p(n_A \geq 2 \cup n_B \geq 2)$  is the probability that at least one of the two protagonists has more than one photon, i.e.

$$p(n_A \geq 2 \cup n_B \geq 2) = \text{tr} \rho_{n_A \geq 2 \cup n_B \geq 2}. \quad (\text{A7})$$

$S$  is thus upper bounded by

$$S \leq S^{\max}(p(n_A \geq 2 \cup n_B \geq 2)) \quad (\text{A8})$$

$$= \frac{16}{\sqrt{2\pi}} \Re \left[ \langle 01 | \rho_{n_A \leq 1 \cap n_B \leq 1} | 10 \rangle \right]$$

$$+ \frac{8}{\pi} \left( \Re \left[ \langle 20 | \rho_{\text{coh}} | 11 \rangle \right] + \Re \left[ \langle 02 | \rho_{\text{coh}} | 11 \rangle \right] \right)$$

$$+ 2\sqrt{2} \times p(n_A \geq 2 \cup n_B \geq 2).$$

Needless to say, separable states are physical states. They are thus represented by positive matrices with a trace (tr) equal to one. Furthermore, the Peres-Horodecki criterion [1, 2] states that for any separable state  $\rho_{\text{sep}}$ , its partial transpose  $\rho_{\text{sep}}^{T_B}$  has non-negative eigenvalues. The maximum value of  $S^{\max}$  over the set of separable states, is thus upper bounded by the result of the following optimization, which we call  $S_{\text{sep}}^{\max}$ .

$$\max_{\rho \in \{|0\rangle, |1\rangle, |2\rangle\}^{\otimes 2}} : S^{\max}(p(n_A \geq 2 \cup n_B \geq 2)) \quad (\text{A9})$$

$$\text{s. t.} : \rho \geq 0$$

$$\text{tr}(\rho) \leq 1$$

$$\rho^{T_B} \geq 0$$

$$\sum_{i,j=0}^1 p_{ij} = 1 - p(n_A \geq 2 \cup n_B \geq 2).$$

where  $p_{ij} = \langle ij | \rho | ij \rangle$ . The constraint  $\text{tr}(\rho) \leq 1$  comes from the fact that the optimization can be performed over finite dimension ( $9 \times 9$ ) matrices that can either represent a physical state or that can be obtained by local projections of states spanning Hilbert spaces with a larger dimension. The above program is a linear optimization with semidefinite positive constraints. It can thus be efficiently solved numerically [3]. The result of the optimization  $S_{\text{sep}}^{\max}$  is shown in Fig. 2 (main text) as a function of  $p(n_A \geq 2 \cup n_B \geq 2)$ . If a physical state that satisfies the last condition leads to a  $S$  value larger than  $S_{\text{sep}}^{\max}$ , one can conclude that its partial transpose has at least one negative eigenvalue and hence, the state is entangled.

### 3. General procedure to follow for witnessing single-photon entanglement

Below, we present the procedure to follow in order to conclude about the presence of entanglement with the proposed witness.

- Firstly, the local photon number distributions  $p(n_a = 0), p(n_b = 0), p(n_a = 1), p(n_b = 1) \dots$  are accessed using local phase-averaged quantum state tomography.

- The joint probability  $p(n_a \geq 2 \cup n_b \geq 2)$  defined by

$$p(n_a \geq 2) + p(n_b \geq 2) - p(n_a \geq 2 \cap n_b \geq 2)$$

is then upper bounded by

$$p^* = 2 - p(n_a = 0) - p(n_a = 1)$$

$$- p(n_b = 0) - p(n_b = 1).$$

- Thirdly,  $p^*$  is used to obtain the separable bound  $S_{\text{sep}}^{\max}(p^*)$  deduced from the following optimization

$$\max_{\rho \in \{|0\rangle, |1\rangle, |2\rangle\}^{\otimes 2}} : S^{\max}(p^*)$$

$$\text{s. t.} : \rho \geq 0$$

$$\text{tr}(\rho) \leq 1$$

$$\rho^{T_B} \geq 0$$

$$\sum_{i,j=0}^1 p_{ij} \geq 1 - p^*. \quad (\text{A10})$$

Alternatively,  $S_{\text{sep}}^{\max}(p^*)$  can simply be obtained from Fig. 2 (main text) because  $S_{\text{sep}}^{\max}$  is a monotonically increasing function of  $p(n_a \geq 2 \cup n_b \geq 2)$ . Both methods provide an upper bound on  $S_{\text{sep}}^{\max}(p(n_a \geq 2 \cup n_b \geq 2)) \leq S_{\text{sep}}^{\max}(p^*)$ .

- Fourthly, the CHSH value is measured. In principle, this is done by proposing Alice and Bob to randomly choose measurements among  $\{X_{\varphi_A^1}, X_{\varphi_A^2}\}$  and  $\{X_{\varphi_B^1}, X_{\varphi_B^2}\}$  respectively and to subsequently compute the CHSH polynomial. However, since  $\Delta\varphi^{11} + \pi = \Delta\varphi^{22}$  and  $\Delta\varphi^{12} = \Delta\varphi^{21}$ ,  $S_{\text{obs}}$  can be obtained in practice from measurements performed with two phase differences ( $\Delta\varphi^{11}$  and  $\Delta\varphi^{12}$ ) only, through

$$S_{\text{obs}} = 2E_{X_{\varphi_A^1}, X_{\varphi_B^1}} + 2E_{X_{\varphi_A^1}, X_{\varphi_B^2}}. \quad (\text{A11})$$

- Finally,  $S_{\text{obs}}$  and  $S_{\text{sep}}^{\max}(p^*)$  are compared. If  $S_{\text{obs}} > S_{\text{sep}}^{\max}(p^*)$  (which implies that  $S_{\text{obs}} > S_{\text{sep}}^{\max}(p(n_a \geq 2 \cup n_b \geq 2))$ ), one concludes that the measured state is entangled. Otherwise, we cannot form a conclusion, the state can either be separable or entangled.

Note that the optimization (A10) does not take full advantage of the individually measured probabilities  $p(n_A = j)$  ( $p(n_B = j)$ ) of having  $j$  photons in Alice's (Bob's) mode. The knowledge of these probabilities can be used to constrain the set of separable states over which  $S^{\max}$  is to be optimized further, and thus provide a tighter bound  $S_{\text{sep}}^{\max}$ . This can be done through the following optimization program:

$$\begin{aligned}
\max_{\rho \in \{|0\rangle, |1\rangle, |2\rangle\}^{\otimes 2}} & : S^{\max}(p^*) & (\text{A12}) \\
\text{s. t.} & : \rho \geq 0 \\
& \rho^{T_B} \geq 0 \\
& \sum_{i,j=0}^1 p_{ij} \geq 1 - p^* \\
& \sum_{j < 2} p_{ij} \leq p(n_A = i) \quad \forall i < n \\
& \sum_{i < 2} p_{ij} \leq p(n_B = j) \quad \forall j < n
\end{aligned}$$

In section B 4 the separable bounds related to the experiment is computed using this last optimization.

## Appendix B: Experimental details

### 1. Heralded creation of single-photon entanglement

A continuous-wave frequency-doubled Nd:YAG laser (Diabolo, Innolight) pumps a triply-resonant type-II phase-matched optical parametric amplifier based on a KTP crystal to generate below threshold, a two-mode squeezed state [4]. The created modes are orthogonally polarized and are deterministically separated at the output of the amplifier. One of the two modes is sent to a single-photon detector (superconducting single-photon detector, with a quantum efficiency of 7% at 1064nm) after filtering of the non-degenerate modes. A detection event ideally heralds the generation of a single-photon state on the twin mode. The heralding rate is around 30 kHz. (See [5] for more details about the source). By controlling the polarization of the heralded photon via a half-wave plate and by subsequently sending it into a polarizing beam splitter (PBS), one gets a versatile source producing states of the form

$$|\psi(\theta)\rangle_{AB} = \cos(2\theta)|0\rangle_A|1\rangle_B + \sin(2\theta)|1\rangle_A|0\rangle_B \quad (\text{B1})$$

where  $\theta$  is the angle of the half-wave plate relative to the axis of the PBS. For  $\theta = 0^\circ$ , the created state is separable, whereas for  $\theta = 22.5^\circ$  it becomes maximally entangled. This source is thus particularly well suited to test the proposed entanglement witness.

### 2. Homodyning

Each spatial mode is then detected using an independent homodyne detection. The required local oscillators are obtained by impinging a bright beam into the second input of the PBS. The phase of Alice's local oscillator is controlled relative to Bob's one by choosing appropriately the polarization of the bright beam just before the PBS [6]. To meet the witness requirements, a phase averaging is realized by sweeping a piezoelectric transducer located on the path of the bright beam before the PBS. The overall efficiency of each homodyne detection is 85%, including the quantum efficiency of the photodiodes (Fermionics 500), mode overlap and electronic noise [7].

### 3. Data acquisition

For each heralding event, Alice and Bob perform a quadrature measurement and the corresponding result is extracted from homodyne photocurrents. 200000 events are accumulated for each relative phase  $\Delta\varphi^{11} = \frac{\pi}{4}$  and  $\Delta\varphi^{12} = -\frac{\pi}{4}$ .  $S_{obs}$  is then deduced from Eq. (A11). The same results are also used to compute the local photon number distributions by phase-averaged quantum state tomography with the MaxLike algorithm [8]. Table 5 shows the results for various angles  $\theta$ .

### 4. Error estimations

Several errors have been taken into account. Firstly, statistical errors affect the measured value of the CHSH polynomial  $S_{obs}$ . These errors are estimated in a standard way by using the central limit theorem. They are basically very small (see Table 5) because they were deduced from 200000 results.

Secondly, the accuracy with which the relative phase  $\Delta\varphi^{\ell\ell}$  between Alice & Bob's measurements is estimated to be  $1^\circ$ . This means that when Alice and Bob choose measurement settings, e.g. corresponding ideally to the quadratures  $X_{\varphi_A^1} - X_{\varphi_B^1}$ , the relative phase  $\Delta\varphi^{11}$  might not be exactly equal to  $\frac{\pi}{4}$  as it should be, but satisfies  $\Delta\varphi^{11} = \frac{\pi}{4} + \epsilon^{11}$  where  $-1^\circ \leq \epsilon^{11} \leq 1^\circ$ .

Thirdly, errors also affect the local photon-number probability distributions, which are estimated using the phase-averaged homodyne measurements and the maximum-likelihood reconstruction algorithm [8]. Evaluating these errors is a not trivial task. One can use the Cramer-Rao bound which is valid in the limit of an infinite number of measurements. However this only considers the statistical error and thus omits more practical aspects, including the truncation of the Fock space, numerical errors and the algorithm convergence. Instead, we use a simpler method for estimating the overall error. The tomography that we use to access the local photon number distributions leaves us with

angle	Alice						Bob						$p^*$		$S_{\text{obs}}$		$S_{\text{sep}}^{\text{max}}$
	$p_{\text{0}}$	error	$p_{\text{1}}$	error	$p_{>1}$	error	$p_{\text{0}}$	error	$p_{\text{1}}$	error	$p_{>1}$	error	$p^*$	error	$S_{\text{obs}}$	error	$S_{\text{sep}}^{\text{max}}$
0	<b>99.8</b>	0.1	<b>0.2</b>	0.1	<b>0.01</b>	0.01	<b>30.6</b>	0.2	<b>65.4</b>	0.3	<b>3.94</b>	0.19	<b>3.9</b>	0.262	<b>0.104</b>	0.001	0.235
5	<b>98.9</b>	0.2	<b>1.1</b>	0.2	<b>0.06</b>	0.04	<b>30.6</b>	0.2	<b>65.5</b>	0.3	<b>3.84</b>	0.20	<b>3.9</b>	0.258	<b>0.353</b>	0.003	0.355
10	<b>92.9</b>	0.2	<b>7.0</b>	0.2	<b>0.10</b>	0.06	<b>36.9</b>	0.2	<b>60.4</b>	0.3	<b>2.70</b>	0.18	<b>2.8</b>	0.274	<b>0.776</b>	0.004	0.643
15	<b>83.6</b>	0.2	<b>16.1</b>	0.2	<b>0.32</b>	0.10	<b>45.6</b>	0.2	<b>52.1</b>	0.3	<b>2.28</b>	0.17	<b>2.6</b>	0.294	<b>1.085</b>	0.004	0.893
20	<b>72.3</b>	0.2	<b>27.2</b>	0.3	<b>0.54</b>	0.13	<b>55.5</b>	0.2	<b>43.2</b>	0.3	<b>1.26</b>	0.17	<b>1.8</b>	0.314	<b>1.289</b>	0.004	1.017
22.5	<b>65.0</b>	0.2	<b>34.0</b>	0.3	<b>0.95</b>	0.16	<b>63.1</b>	0.2	<b>35.8</b>	0.3	<b>1.06</b>	0.16	<b>2.0</b>	0.338	<b>1.326</b>	0.004	1.060
25	<b>59.4</b>	0.2	<b>39.3</b>	0.3	<b>1.33</b>	0.17	<b>67.3</b>	0.2	<b>31.8</b>	0.3	<b>0.90</b>	0.13	<b>2.2</b>	0.312	<b>1.330</b>	0.004	1.072
30	<b>48.3</b>	0.2	<b>49.6</b>	0.3	<b>2.17</b>	0.17	<b>78.2</b>	0.2	<b>21.3</b>	0.2	<b>0.47</b>	0.10	<b>2.6</b>	0.292	<b>1.235</b>	0.004	0.989
35	<b>38.8</b>	0.2	<b>58.4</b>	0.3	<b>2.77</b>	0.18	<b>89.5</b>	0.2	<b>10.5</b>	0.2	<b>0.05</b>	0.06	<b>2.8</b>	0.283	<b>0.951</b>	0.004	0.755
40	<b>32.2</b>	0.2	<b>64.2</b>	0.3	<b>3.66</b>	0.20	<b>96.9</b>	0.2	<b>3.1</b>	0.2	<b>0.05</b>	0.04	<b>3.7</b>	0.265	<b>0.527</b>	0.003	0.493
45	<b>30.1</b>	0.2	<b>66.3</b>	0.3	<b>3.59</b>	0.19	<b>99.7</b>	0.1	<b>0.2</b>	0.1	<b>0.02</b>	0.01	<b>3.6</b>	0.224	<b>0.112</b>	0.001	0.233

FIG. 5: Results of local measurements versus the angle of the half-wave plate relative to the axis of the PBS. The table on the left gives the photon number distribution in Alice's location. ( $p_{\text{0}}$ ,  $p_{\text{1}}$ ,  $p_{>1}$  denote the probability that zero ( $p(n_A = 0)$ ), one ( $p(n_A = 1)$ ) and more than one photon ( $p(n_A \geq 2)$ ) occupy Alice's mode. The second table gives Bob's results. The two last tables give an upper bound on the probability that at least one of the two protagonists gets more than one photon ( $p(n_A \geq 2 \cup n_B \geq 2)$ ) and the observed CHSH value  $S_{\text{obs}}$ .)

the diagonal elements of an estimated density matrix  $\rho_{\text{estimate}}$ . Using this matrix, we simulate the quadrature data, then apply the MaxLike algorithm to reconstruct the diagonal elements of a simulated density matrix  $\rho_{\text{simul}}$ . The approach is repeated 200 times, always from the same initial state  $\rho_{\text{estimate}}$ . This generates a random set of 200 data points for each local probability  $p(n_A = 0), p(n_B = 0), p(n_A = 1), p(n_B = 1) \dots$  and the corresponding standard deviation provides the desired error  $\delta p(n_A = 0), \delta p(n_B = 0), \delta p(n_A = 1), \delta p(n_B = 1) \dots$

We now show how the errors on the measurement angles  $\epsilon^{\ell\bar{\ell}}$  and on the local photon-number probability distributions  $\delta p(n_A = i), \delta p(n_B = j)$  have been taken into account in the calculation of the separable bound  $S_{\text{sep}}^{\text{max}}$ . Since, in practice, it is necessary to measure two correlators only, the errors are the same for  $\Delta\varphi^{11}$  and  $\Delta\varphi^{22}$  and for  $\Delta\varphi^{12}$  and  $\Delta\varphi^{21}$ , namely

$$\begin{aligned}\Delta\varphi^{11} &= -\frac{\pi}{4} + \epsilon^{11}, \Delta\varphi^{22} = \frac{3\pi}{4} + \epsilon^{11}, \\ \Delta\varphi^{12} &= \Delta\varphi^{21} = \frac{\pi}{4} + \epsilon^{12}.\end{aligned}$$

These erroneous measurement angles yield to an upper bound  $S^{\text{max}}$  (which replaces the one in Eq. (A8)) given by

$$\begin{aligned}S &\leq S^{\text{max}}(p(n_A \geq 2 \cup n_B \geq 2), \epsilon^{11}, \epsilon^{12}) \\ &= \frac{4}{\pi} \left( \Re[\langle 10|\rho|01\rangle] \times C - \Im[\langle 10|\rho|01\rangle] \times D \right) \\ &\quad + \frac{4}{\sqrt{2}\pi} \Re[\langle 20|\rho|11\rangle + \langle 11|\rho|02\rangle] \times C \\ &\quad - \frac{4}{\sqrt{2}\pi} \Im[\langle 20|\rho|11\rangle + \langle 11|\rho|02\rangle] \times D \\ &\quad + 2\sqrt{2} \times p(n_A \geq 2 \cup n_B \geq 2)\end{aligned}\quad (\text{B2})$$

where  $\Im$  denotes the imaginary part and

$$\begin{aligned}C &= 2 \left( \cos(\epsilon^{11} - \frac{\pi}{4}) + \cos(\epsilon^{12} + \frac{\pi}{4}) \right), \\ D &= 2 \left( \sin(\epsilon^{11} - \frac{\pi}{4}) + \sin(\epsilon^{12} + \frac{\pi}{4}) \right).\end{aligned}$$

$S^{\text{max}}$  can now be optimized over the set of separable states, as before. If one takes into account the local photon number probability distribution and the errors as well, one ends up with the following optimization problem

$$\begin{aligned}\max : & S^{\text{max}}(p^*, \epsilon^{11}, \epsilon^{12}) \\ \text{s.t.} : & \rho \geq 0 \\ & \text{tr}(\rho) \leq 1 \\ & \rho^{T_B} \geq 0 \\ & -1^\circ \leq \epsilon^{11}, \epsilon^{12} \leq +1^\circ \\ & p_{00} + p_{10} + p_{01} + p_{11} \geq 1 - p^* - \delta p^* \\ & p_{00} + p_{01} + p_{02} \leq p(n_A = 0) + \delta p(n_A = 0) \\ & p_{10} + p_{11} + p_{12} \leq p(n_A = 1) + \delta p(n_A = 1) \\ & p_{20} + p_{21} + p_{22} \leq p(n_A > 1) + \delta p(n_A > 1) \\ & p_{00} + p_{10} + p_{20} \leq p(n_B = 0) + \delta p(n_B = 0) \\ & p_{01} + p_{11} + p_{21} \leq p(n_B = 1) + \delta p(n_B = 1) \\ & p_{02} + p_{12} + p_{22} \leq p(n_B > 1) + \delta p(n_B > 1)\end{aligned}\quad (\text{B3})$$

In addition to errors, we emphasize that the previous optimization uses the knowledge of each local photon number probability  $p(n_A = 0), p(n_A = 1) \dots$ . This provides a tighter separable bound as compared to the optimization summarized in Eq. (A10).

Note that the optimization (B3) is non-linear in  $\epsilon_{11}$  and  $\epsilon_{12}$ . Hence, the result cannot be obtained directly with standard semidefinite solvers. However, we could check numerically that the maximum value of  $S_{\text{sep}}^{\text{max}}(p^*, \epsilon^{11}, \epsilon^{12})$  is obtained for the extremal choice

$\epsilon_{11} = 1^\circ$ ,  $\epsilon_{12} = -1^\circ$ . This can be understood intuitively since this choice brings the settings closer to each other and thus, helps in increasing the CHSH value. Note that the linearity of the optimization is recovered once

the values of  $\{\epsilon_{11}, \epsilon_{12}\}$  are fixed. The results of the optimization for  $\epsilon_{11} = 1^\circ$  and  $\epsilon_{12} = -1^\circ$  are shown in Fig. 4 (main text).

- 
- [1] A. Peres, Phys. Rev. Lett. **77**, 1413 (1996).  
 [2] M. Horodecki, P. Horodecki, and R. Horodecki, Phys. Lett. A **223**, 1 (1996).  
 [3] S. Boyd and L. Vandenberghe, *Convex optimization* Cambridge University Press (2004).  
 [4] J. Laurat, T. Coudreau, G. Keller, N. Treps, C. Fabre, Phys. Rev. A **70**, 042315 (2004).  
 [5] O. Morin, V. D'Auria, C. Fabre, J. Laurat, in preparation.  
 [6] J. Laurat, T. Coudreau, G. Keller, N. Treps, C. Fabre, Phys. Rev. A **71**, 022313 (2005).  
 [7] R. Kumar, E. Barrios, A. MacRae, E. Cairns, E.H. Huntington, A.I. Lvovsky, eprint arXiv:1111.4012.  
 [8] A.I. Lvovsky, M.G. Raymer, Rev. Mod. Phys. **81**, 299 (2009).